

POROSITY EVALUATION OF PYROLYTIC CARBON IN TRISO-COATED FUEL PARTICLES BY THE DEPTH-SENSING INDENTATION METHOD

Kyeong Hwan Park, Ji Yeon Park[‡], Weon-Ju Kim, Young Woo Lee and Jong Hwa Chang

Korea Atomic Energy Research Institute, P.O. Box 105, Yuseong, Daejeon 305-600, Republic of Korea

Tel: 82-42-868-2311, Fax: 82-868-8346

ABSTRACT

The coating layers surrounding the fuel kernels in spherical TRISO coated particles, consisting of pyrolytic carbon (PyC) and silicon carbide (SiC) layers, act as a pressure vessel that retains the fission products. We attempted a depth-sensing indentation method to obtain the porosity of the PyC layers by using various porosities in sphere coated particles by investigating several reported equations, which are widely used to describe the relation between the elastic moduli and the porosity. The elastic modulus was obtained by indenting the optionally and fully coated TRISO fuel particles. By using the measured elastic moduli, the porosities were calculated by the reported equations. The porosity obtained by the present method was converted to a density value. The results were analyzed by comparing them with that from different techniques including pycnometry, a dimension measurement and the sink-float method and by observing the microstructures.

INTRODUCTION

One of the critical issues of the gas-cooled reactor is the TRISO coated fuel, which contains a UO₂ kernel, pyrolytic carbon (PyC) and silicon carbide (SiC) layers [1]. Accurate estimates of the out-of-pile and in-pile material properties of the coated particles are critical for the development of robust and reliable fuel performance models [2]. Many properties at each layer are of interest for designing the TRISO fuel particle, which include the thickness, uniformity, density, porosity, microstructure, permeability and the anisotropy, etc. Even though various measuring techniques have been applied to evaluate the properties of the coated layers in the TRISO coated particles, better evaluation methods will be continuously requested to obtain advanced data. The present

study is focused on the pyrolytic carbon (PyC) layer in the TRISO system to assess its' porosity and density. Normally the densities of the coated layers are measured by a gas pycnometer, a mercury porosimeter, and a density gradient column (sink-float method). A pycnometer is a vessel with a precisely known volume. A gas pycnometer operates by detecting the pressure change resulting from the displacement of a gas by a solid object. The gas law, $PV = nRT$ is applied to determine the volume of the unknown. Mercury is a non-wetting liquid that must be forced into a pore by the application of an external pressure. In a porosimeter, when an object is surrounded by mercury, the mercury forms a closely fitting liquid envelope around the object. How closely the mercury conforms to the surface features of the object depends on the pressure applied. At some pressures, the mercury begins to enter the pores, cracks, crevices, and voids of the sample. Therefore, a mercury porosimeter can measure the bulk, envelope and skeletal volumes. The sink-float method measures the depth to which solid fragments sink in a column of a liquid possessing a known density gradient [3]. But these methods have some limitations like an accuracy and difficulty of sample preparation. Two types of PyC including dense and porous layers constitute a fully coated TRISO fuel particle. In order to use the density gradient column, the interested PyC layer has to be separated from the TRISO system. A possible separation method is that the fuel should be crushed and then the remaining materials optionally collected by a manual operation. At that time, the PyC seems to undergo an enormous compressive stress with its breaking-off. In the case of a gas pycnometer and a mercury porosimeter to measure the density of the OPyC, after the density measurement of the fully coated TRISO fuel particles, all the particles are recovered, cleaned, heated at a low temperature to remove the residual mercury (in the case

[‡] Corresponding Author : Ji Yeon Park, jypark@kaeri.re.kr

of a porosimeter), and heated in air at over 750 °C to remove the OPyC layer. The mass and volume of the particles with the OPyC removed is then measured and the mass and volume of the OPyC is calculated by a subtraction method. Note that the density and the porosity of the buffer, inner PyC and SiC layer in the fully coated TRISO particles can not be measured by using a pycnometer and a porosimeter. The density measurement by using the above methods has the possibility of analyzing the collected PyC together with additional materials like a kernel and SiC splits. It could be a reason for the non-reliable data by overestimating the PyC density due to a simultaneous analysis of the additional materials. Another method for the density measurement is to divide the mass by the volume of the interested PyC layer in the TRISO fuel particles, where the mass and the volume are determined by a weighing and image analysis of the cross-sections, respectively. The dimension measurements of a TRISO fuel cross-section also have some difficulties because of a time-consuming process and a lack of a standard experimental procedure. In addition, a dimensional measurement can not be applicable to a fully coated TRISO particle because it is difficult to determine the precise mass of the one of the interested layers.

Therefore, we attempted a new approach to obtain the porosity of the PyC layers by maintaining the constitution of the completed TRISO fuel particles. In the mean time, it has been reported that the porosity has influenced the elastic moduli of materials in many studies. Especially, the elastic modulus of highly pure PyCs with the same microstructural morphology is mainly dependent on its porosity [4-8]. Namely, the porosity of the PyC layer can be determined by measuring the elastic modulus. It has been reported that the elastic modulus of materials can be determined by several techniques such as a tensile test, an acoustic microscopy, an impulse excitation technique and a nano-indentation test [9]. A depth-sensing indentation is a useful method for an elastic modulus determination of a material with a small size and a complicated shape like the TRISO fuel particle. A proper equation was chosen from the references, which was used to describe the relation between the elastic modulus and the porosity. The porosities derived from the measured elastic moduli could be converted to density values. Then, the values were compared with that calculated by other methods and the microstructures were investigated.

NOMENCLATURE

A_c	Contact area of diamond indenter
C	Compliance
E	Elastic modulus (GPa)
E_0	Elastic modulus at porosity zero
E_r	Reduced elastic modulus (GPa)
E_s	Elastic modulus of test sample
E_i	Elastic modulus of diamond indenter tip
h_c	Contact depth of diamond indenter
h_{max}	Depth at maximum load
h_r	Residual depth of diamond indenter
H	Hardness
P	porosity (%)
P_{max}	Maximum indentation load

S	Stiffness
ε	Geometrical constant of the indenter, 0.75
ν	Poisson's ratio
ν_s	Poisson's ratio of test sample
ν_i	Poisson's ratio of diamond indenter tip
β	Geometrical constant of the indenter, 1.034

MATERIALS

The coated particles used for the porosity measurement were deposited onto the ZrO₂ kernels as surrogates for the UO₂ particles in a fluidized bed CVD coater. In this work, a graphite tube of 25 mm in inner diameter with an inlet nozzle of 3 mm at the base of a 60° cone was used as the bed tube. At the deposition temperatures, 14 g of ZrO₂ particles were put into the coater from the top of the graphite tube in the presence of an Ar flow from the bottom of the coater. After assuring the fluidization of the particles through a quartz window, reactants were put into the coater to produce a coating layer on the particles fluidized in the coater. The input gases for the depositions of the buffer, IPyC and OPyC were C₂H₂/Ar and C₂H₂/C₃H₆/Ar, respectively. For the buffer coating, the concentration of C₂H₂ was set to 70 %. The total gas flow rate was varied from 1600 to 2500 sccm at the coating temperatures of 1250 °C and 1300 °C. The IPyC and OPyC layers were coated by using the predetermined coating gas concentrations and the gas flow rates at 1300 °C. Different microstructures of the PyC can be obtained as a function of the total gas flow rates and the coating temperatures.

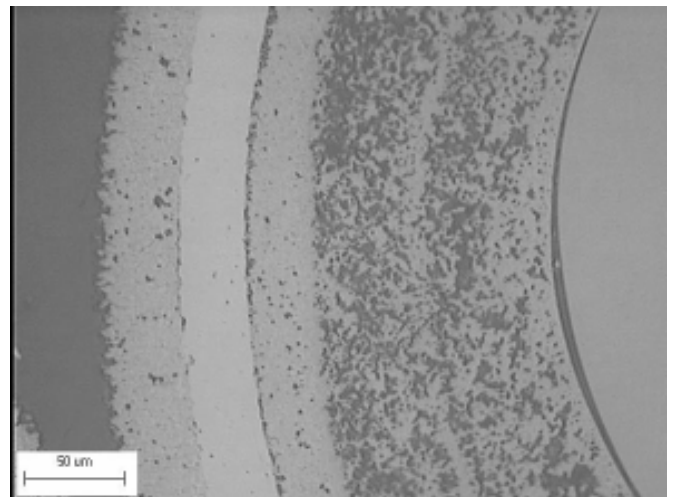


Fig. 1 The cross-sectional image of the completed TRISO coated particle by optical microscope

After a deposition of the coating layers, the TRISO-coated particles were mounted in an epoxy resin and polished down to close the middle plane of the particles. To evaluate the porosity, the PyC layers with various porosities were optionally coated onto a ZrO₂ kernel (See Fig 6, TR-A, B and C). Microstructure of the fully coated particle was observed for a polished cross-section by using an optical microscopy (see Fig. 1).

DEPTH-SENSING INDENTATION

The depth-sensing indentation test was carried out with a nano-indentation device (NanoTest, Micro Materials Ltd.) and a Berkovich diamond tip. It is known that a precise determination of the elastic moduli is a primary factor for measuring the porosity of the PyC layer in the TRISO particles. The importance of an accurate indenter shape calibration has been discussed as an overestimation of the elastic modulus data has been reported in the case of a non-calibrated indenter tip [10].

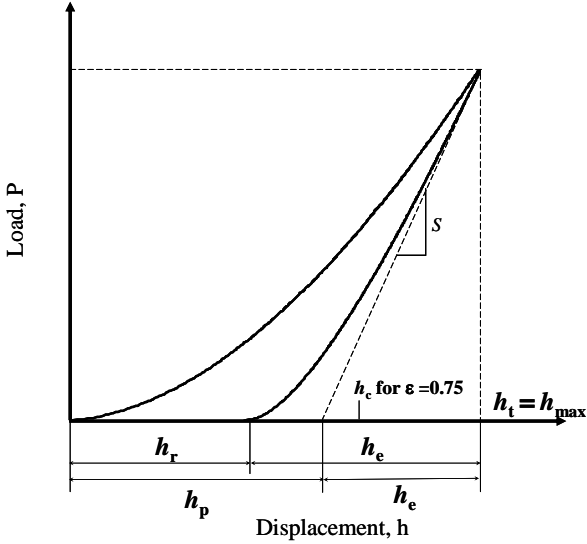


Fig. 2 The load-depth curve obtained from one complete indentation test.

The experimental parameters, such as the maximum load (P_{\max}), the depth at the maximum load (h_{\max}) and the initial unloading contact stiffness (S), for the hardness and the modulus can be determined from a load-displacement curve as shown in Fig. 2. The reduced indentation modulus, E_r , is defined as:

$$E_r = \frac{\sqrt{\pi} S}{2 \beta \sqrt{A_c}}$$

where E_r is

$$\frac{1}{E_r} = \frac{1 - \nu_s^2}{E_s} + \frac{1 - \nu_i^2}{E_i}$$

and, S is the contact stiffness between the indenter and the specimen, that is the derivative of the first 1/3 of the unloading curve, β is a geometrical constant of the indenter. E and ν are the Young's modulus and the Poisson's ratio of the materials, respectively, where the subscripts s and i indicate the properties of the specimen and the indenter. At less than a micrometer, however, deviations of the hardness and the modulus are significant due to a tip rounding or an indentation size effect. For complementing this problem, the calibration method proposed by Oliver and Pharr [11] was used in this work. For a calibration of the area function of an indenter tip, quartz was used. Hardness, H , is defined as follows:

$$H = \frac{P_{\max}}{A(h_c)}$$

where P_{\max} is the maximum load and A is the projected contact area between the indenter and the specimen at the maximum force. $A(h_c)$ is determined from the load-displacement curve and the area function of the indenter, which is dependent on the contact depth h_c and the shape of an indent tip. The contact depth is also obtained from the load-displacement curve by using

$$h_c = h_{\max} - \varepsilon(h_{\max} - h_r)$$

where ε is a geometric constant, 0.75 for a Berkovich indenter tip [11]. In order to calibrate the area function of a diamond indenter, a set of indentations was performed with quartz and then the unloading stiffness, S , was calculated for each indent by assuming a perfect indenter shape with a face angle of 65.0° . The projected area was estimated from the

Table 1. Empirical or semi-empirical expressions for the dependency of the elastic modulus on the porosity, cited in reference [12]

Author	Expression	Description
Knudsen	$E = E_0 \exp(-bP)$	No satisfaction of the boundary condition, $E = 0$ for $P = 1$
Wang	$E = E_0 \exp[-(bP + cP^2)]$	For materials composed of uniform-sized spherical particles packed in cubic array
Phani-Niyogi	$E = E_0(1 - aP)^n$ $E = E_0 \exp[-(bP + cP^2 + dP^3 + \dots)]$	For higher porosity, a relation with polynomial exponent.
Ishai-Cohen	$E = E_0(1 - P^{2/3})$	A two-phase model of cubic inclusion within a cubic matrix.
Coble-Kingery	$E = E_0(1 - 1.91P + 0.91P^2)$	Boundary condition $E = 0$ at $P = 1$.
Hasselmann	$E = E_0 \{1 + AP / [1 - (A + 1)P]\}$	
Czeremskoy	$E = E_0(1 - P) / (1 + kP)$	k for heterogeneous system containing non-intersected pores

stiffness values obtained from the load-displacement curve using:

$$A(h_c) = C_1 h_c^2 + C_2 h_c + C_3 h_c^{1/2} + C_4 h_c^{1/4} + \dots + C_9 h_c^{1/128}$$

where C_1 is the area function for a perfect Berkovich indenter, and C_2 through C_9 are constants. The area function is determined by plotting the calculated contact area, A against the depth h_c . The procedure for calibrating an area function proposed by Oliver and Pharr [11] was applied to a Berkovich indenter tip. The indentation was tested with the maximum penetration depth of a diamond tip (about 1000 to 1500 nm) in a device in order to reflect the influence of the pores to the utmost in a pyrolytic carbon layer.

RELATION BETWEEN ELASTIC MODULUS AND POROSITY

The porosity affects the elastic modulus (E), where the E is always decreasing with an increasing porosity P . The relation between the property and the porosity was studied for various materials and models [4-8]. A dependency of the elastic modulus, E on the porosity, P has been proposed by many researchers. Krzesinska [12] pointed out that the helpful arrangement of the elastic modulus-porosity relations was provided by empirical equations by attaching boundary conditions. Table 1 cited from the reference shows useful information on the relation of the elastic modulus-porosity. The polynomial equation proposed by Coble and Kingery [13] has found a general acceptance in porous ceramic and carbon materials, which have been derived from the Mackenzie expression on the basis of a boundary condition $E = 0$ at $P = 1$.

$$E = E_0(1 - 1.91P + 0.91P^2)$$

where E_0 and P are the elastic modulus of a nonporous material and the volume fraction of the pores, respectively. The relation is valid for materials containing up to a 50 % porosity and having a Poisson's ratio of 0.3. For the purpose of a verification of the porosity values, the porosities were converted to density values from the measured elastic moduli by assuming a 2.2 g/cm³ density of PyC with non-pores.

RESULTS AND DISCUSSIONS

Fig. 3 shows the plots of the load-depth curves of the TRISO structured specimen without a delamination of each layer which is the representative depth-sensing indentation data obtained from a dense PyC (inner PyC) and a porous PyC (buffer). We can see that a highly elastic recovery with no plastic deformation occurred in both PyC layers after an indentation, even at a penetration depth of ~ 1500 nm. The elastic recovery in the PyC layers is clearly confirmed by the microstructure observation after an indentation. The depth sensing indentation test was performed on the polished surface of the fully coated TRISO particles with four

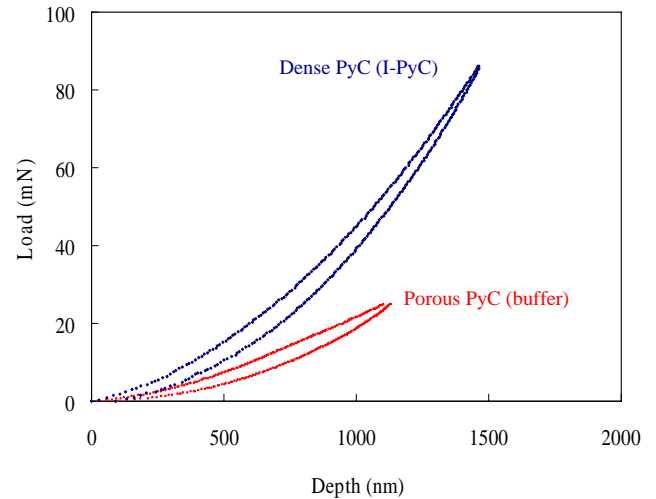


Fig. 3 Load-depth curves of the inner and buffer PyC layer obtained by the depth-sensing indentation test

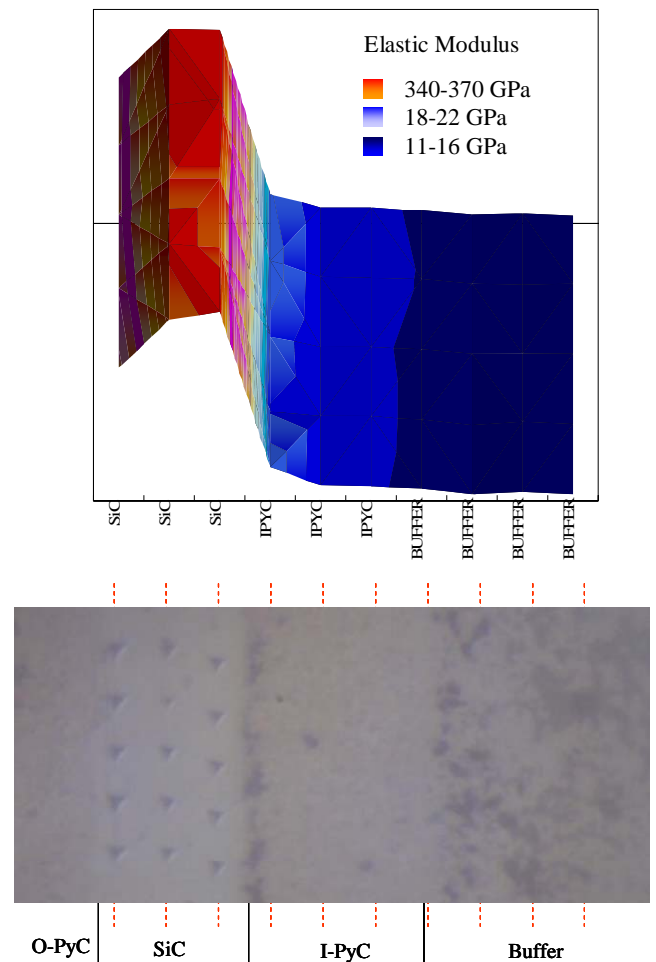


Fig. 4 Elastic modulus of the SiC, I-PyC and buffer layers in the TRISO particle corresponding to the microstructure.

components; outer PyC / SiC / inner PyC / buffer PyC without a delamination of each layer. Fig. 4 shows the distribution of the elastic moduli and the corresponding

indentation impressions. While the indentation impressions were clearly observed in the SiC layer, those in the IPyC and buffer PyC were rarely found. An unclear observation of the indentation impressions seems to have resulted from a full elastic recovery of the PyC layers. As shown in Fig. 4, however, the elastic modulus of each layer can be estimated by this method. The elastic modulus of the inner PyC and the buffer layer exhibit about 22 ± 1 GPa and 12.5 ± 1.5 GPa, respectively.

In the TRISO particles, the thickness of each coated layer is several tens of micrometers. Additionally, the coated layers have complicated structures such as a spherical shape and a four layer bond. Therefore, we have a difficulty to produce the stress-strain curves for an estimation of the elastic modulus of each layer in the TRISO particles. Considering the results shown in Figs. 3 and 4, a depth-sensing indentation is a very easy and simple test method for an evaluation of the elastic modulus of each layer in the TRISO coated particle without a delamination of each layer.

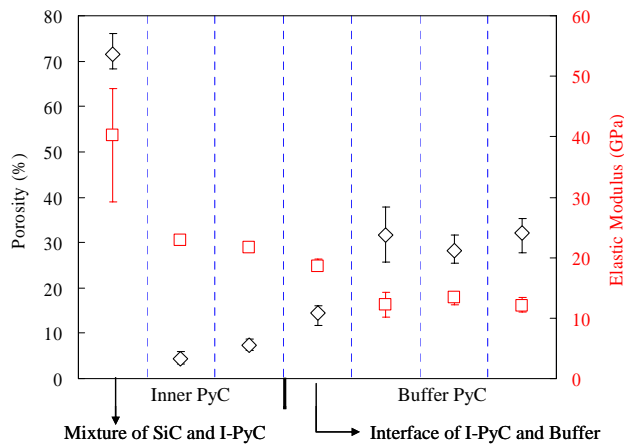


Fig. 5. Porosity (diamond symbol) calculated from the elastic moduli (rectangle symbol) at the inner and buffer PyC.

Fig. 5 shows the calculated porosity of the inner and buffer PyC corresponding to the elastic moduli in Fig. 4. The tendency of the porosity agreed well with microstructure as shown in Fig. 4. The elastic modulus of the SiC layer in Fig. 4, reveals a slightly lower value when compared with that of the reported reference. But, we obtained the sound SiC layer by a careful control of the coating process.

TRISO particles with various microstructures were fabricated by controlling the input gas ratio and the temperature, which provided several types of PyC layers with different porosities. The elastic moduli of the PyC layers were in the range of 8.6 to 22.9 GPa depending on the porosities measured by the depth-sensing indentation tests. The calculated porosities of the corresponding PyC layers were in the range of 43.7 to 4.5 %. The novel method applied in this work has an advantage for obtaining the porosity from a fully coated TRISO particle. In addition, a porosity distribution can be arranged by a data value at each layer in the TRISO particles.

The densities of the PyC layers were measured by various methods such as the sink-float, the dimensional measurement and the gas pycnometer methods, to compare the porosity estimated by the depth-sensing indentation. The various results of the density were obtained depended on the measuring techniques because the different volume at the same specimen is estimated according to the measuring methods. Therefore, the densities were different for the measuring methods used for the same specimen. Especially, this difference is large in a porous specimen. In order to accurately evaluate the density, therefore, a definition of the applied volume is previously considered. Volumes of solid objects are defined by several manners in the American Society for Testing and Materials, ASTM and the British Standards Institute, BSI. The definitions of the densities are listed in Table 2. The representative densities are three types: theoretical, skeletal and bulk densities. It seems that the bulk density has the smallest value because it is calculated by using a bulk volume, which includes the voids within the pieces as well as the voids among the pieces of the particular collection (implied by ASTM D3766). And the skeletal density has the largest value among the measurable densities. The skeletal volume and density can be measured by a gas pycnometry, whereas the bulk, envelope, and skeletal volumes and densities can be obtained by a mercury porosimetry. To verify the indentation-derived density, the

densities of the dense and porous PyC layers coated on the ZrO_2 particles were measured by two different methods with a pycnometer and an optical microscope with an image analyzer. While the pycnometer supplied the skeletal

Table 2. Definitions of various types of densities that follow from the definitions of volume [14, 15].

Density	Definition
Bulk density	The mass of a unit volume of material including both permeable and impermeable voids. (ASTM C 559 – 90) The ratio of the mass of a collection of discrete pieces of solid material to the sum of the volumes of: the solids in each piece, the voids within the pieces, and the voids among the pieces of the particular collection. (ASTM D 3766 – 86)
Envelope density	The ratio of the mass of a particle to the sum of the volumes of: the solid in each piece and the voids within each piece, that is, within close-fitting imaginary envelopes completely surrounding each piece. (ASTM D 3766 – 86)
Skeletal density	The ratio of the mass of discrete pieces of solid material to the sum of the volumes of: the solid material in the pieces and closed (or blind) pores within the pieces. (ASTM D 3766 – 86)
Theoretical density	The ratio of the mass of a collection of discrete pieces of solid material to the sum of the volumes of said pieces, the solid material having an ideal regular arrangement at the atomic level. (ASTM D 3766 – 86)

Table 3 Densities of various types of the PyC layers coated on a ZrO₂ kernel by fluidized bed chemical vapor deposition method.

TRISO Particle ID	Density				Shape Description
	Pycnometer	Optical microscope	Sink-float	Indentation (Standard Deviation)	
TR-A	2.131	2.076	2.048	1.904 (0.037)	Optionally coated and simulated IPyC ZrO ₂ / Dense
TR-B	1.865	1.141	-	1.421 (0.208)	Optionally coated to Buffer layer ZrO ₂ / Porous
TR-C	1.803	1.267	-	1.330 (0.271)	Optionally coated to Buffer layer ZrO ₂ / Porous

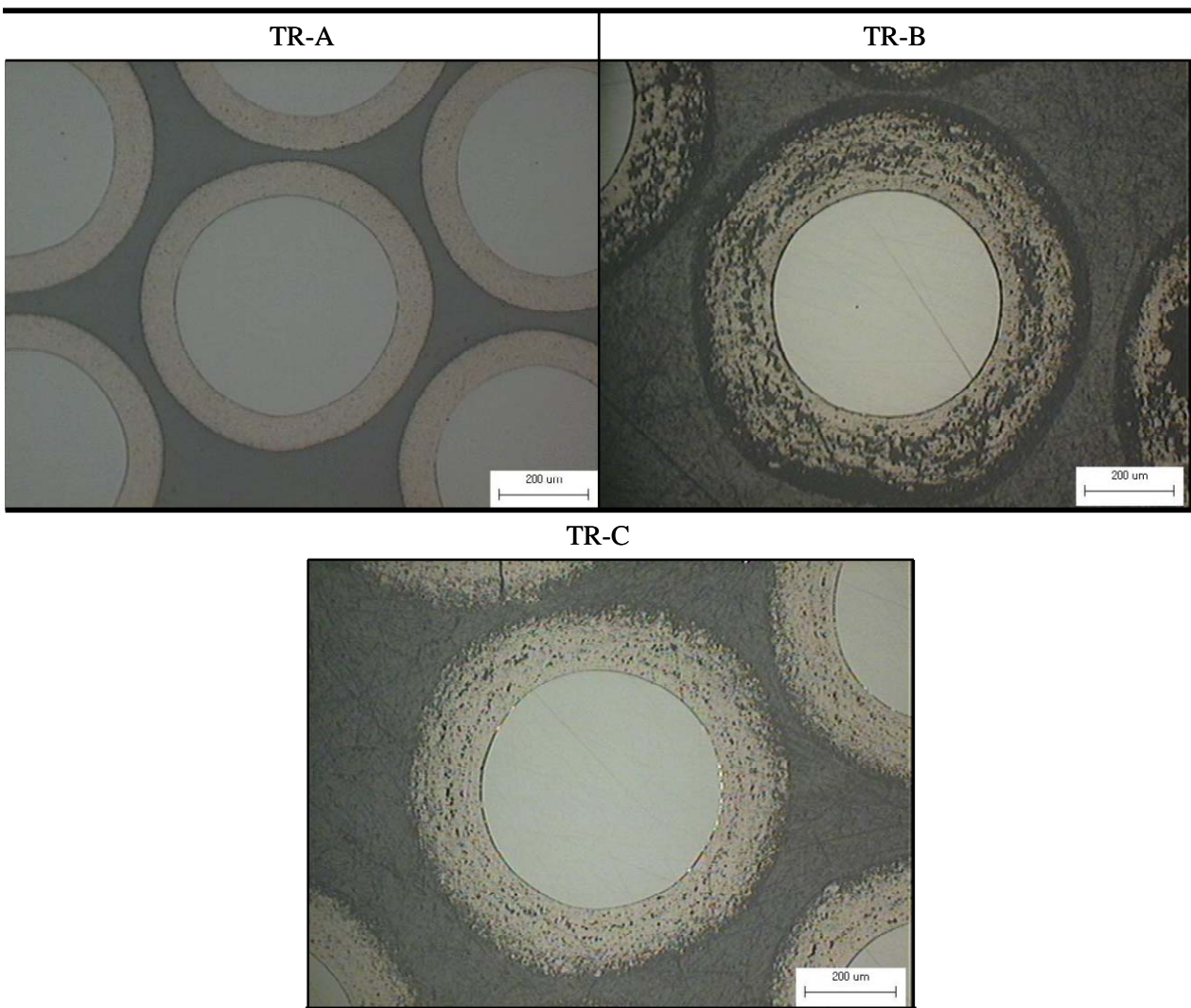


Fig. 6 Micrographs of the various types of the PyC layers coated on ZrO₂ kernels by the fluidized bed chemical vapor deposition method.

densities of both PyCs, the optical microscope supplied the bulk densities. In the optical microscope method, the density

of the PyC layer was estimated by a subtraction of the known ZrO₂ density from the total density including the PyC layer

and a ZrO_2 kernel particle. The optical micrographs were used as a base resource for a volume evaluation of the coated particles in the optical microscope method. These micrographs are projected images which contains the solids parts as well as the voids of a specimen. Therefore, the volumes from the optical microscope are the bulk ones.

Three types of PyC layers with different porosities were prepared by a coating on the ZrO_2 sphere particles and the densities of the PyC layers were measured by different test methods such as the pycnometer, the optical microscope and the indentation methods. The estimated densities of the PyC layers are summarized in Table 3. The corresponding microstructures of the coated particles are described in Fig. 6. For a convenience, the specimens are denoted as TR-A, B and C by considering only the microstructure, the densities of the PyC layers were increased in the following order; TR-B < TR-C < TR-A. That is, this suggests that the optical microscope derived densities of TR-A were the largest ones and that of TR-B were the smallest ones. This agreed with the experimentally estimated ones. As shown in Table 3, however, the different ordered the estimated densities TR-C < TR-B < TR-A were obtained in the pycnometer and the indentation method. In the pycnometer method, helium gas was used as a medium for measuring the unknown volume. This medium gas was penetrated through the open pores and it soaked the surface of the net solid parts of the specimen containing only closed pores. Therefore, the estimated volume by the pycnometer method is different from that by the optical microscope method. This estimated volume is the skeletal volume and density. The bulk volume is larger than the skeletal one because the bulk volume contains the volumes of the solid parts and the closed pores as well as the open pores. Therefore, the skeletal density is larger than the bulk density for the same specimen and the pycnometer derived density is larger than the optical microscope derived one. The density difference between both methods is inferred to increase with an increase of the amounts of the open pores in a specimen. In our estimated results, the similar tendency was obtained as shown in Table 3.

While the densities are estimated based on the apparent properties in the optical microscope method and the pycnometer method, the densities by using the indentation method are produced from a statistical estimation of the directly measured values at the local parts of a specimen. Therefore, the real situations of a specimen are reflected to the data when compared with the previous two methods. But, if a specimen has a lower homogeneity, it may be difficult to produce reliable data. To improve this disadvantage, an optimization for the measuring numbers and the selection of the measuring parts needs to be made. In Table 3, the indentation derived densities of the PyC layers with different porosities are described. The estimated densities by the indentation method showed a similar tendency to those by the pycnometer method although each value was a little smaller than that from the pycnometer method. These results mean that the indentation method is one of the candidates for an easy measurement of the density of the PyC layers in the TRISO particles. Because of a statistical estimation, a deviation of the data is one of the important factors for a

reliability of the data. In our result, a scattering of the data was observed with an increase of the porosity of the PyC layers. Thus the standard deviation of the data from the porous PyC is larger than that from the dense PyC. These deviations may be directly related to the real situations of a specimen such as the pores, imperfections; like micro-cracks and small sized defects, etc. In a porous specimen, production of the exact and reproducible elastic modulus data by the indentation method is not easy because the test data can not be obtained when the diamond tip is indented around and at large pores. In addition, if various imperfections like micro-cracks and small sized defects exist in the load applied zone, a reduction of the elastic modulus will occur. These small imperfections in the PyC layer affect the elastic moduli, while the critical size of a density-affected pore is not well known at present. Therefore, the denser the specimen indicates the higher the reliability of the data.

There are several methods for an evaluation of the density of the PyC layers in TRISO coated particles. The indentation method is a novel approach for an estimation of the density by a simultaneous measurement without delaminations of each layer. In this method, the solid parts and some imperfections like the closed pores and other voids seem to contribute to an estimation of the density. Therefore, the values are equivalent or a little smaller than those by the pycnometer method depending on the porosities of the specimens. To produce more reliable data, an optimization of the evaluation process is needed.

CONCLUSIONS

A new approach was introduced to estimate the densities of the PyC layers in the TRISO coated particles without a delamination of each layer. In this method, the density was estimated by using a known equation for a relation of the porosity versus the elastic modulus after an evaluation of the elastic modulus by the depth sensing indentation method. The estimated densities were a little smaller than the pycnometer derived densities, which seemed to have resulted from the contributions of different amounts of the voids. The difference of the values between the indentation method and the pycnometer method decreased with an increase of the specimen porosity.

REFERENCES

- [1] Wolf, L., Ballensiefen, G., and Fröhling, W., 1975, "Fuel elements of the high temperature pebble bed reactor," *Nuclear Engineering and Design*, Vol. 34, pp. 93-108.
- [2] Petti, D. A., Buongiorno, J., Maki, J. T., Hobbins, R. R. and Miller, G. K., 2003, "Key differences in the fabrication, irradiation and high temperature accident testing of US and German TRISO-coated particle fuel, and their implications on fuel performance," *Nuclear Engineering and Design*, Vol. 222, pp. 281-297.
- [3] Paul, A. W., 2001, "Volume and density determinations for particle technologists" *Technical Article*, Micromeritics Instrument Corporation, <http://www.micromeritics.com/>

- [4] Kaae, J. L., 1971, "Relations between the structure and the mechanical properties of fluidized-bed pyrolytic carbons," *Carbon*, Vol. 9, pp. 291-299.
- [5] Rice, R. W., 1993, "Comparison of stress concentration versus minimum solid area based mechanical property-porosity relations," *Journal of Materials Science*, Vol. 28, pp. 2187-2190.
- [6] Rice, R. W., 1996, "Evaluation and extension of physical property-porosity models based on minimum solid area," *Journal of Materials Science*, Vol. 31, pp. 102-118.
- [7] Phani, K. K., and Niyogi, S. K., 1987, "Young's modulus of porous brittle solids," *Journal of Materials Science*, Vol. 22, pp. 257-263.
- [8] Spriggs, R. M., 1961, "Expression for effect of porosity on elastic modulus of polycrystalline refractory materials, particularly aluminum oxide," *Journal of the American Ceramic Society, Discussions and Notes*, pp. 628-629.
- [9] Bellan, C., Dhers, J., 2004, "Evaluation of Young modulus of CVD coatings by different techniques," *Thin Solid Films*, Vol. 469-470, pp. 214-220.
- [10] Doerner, M. F. and Nix, W. D., 1986, "A method for interpreting the data from depth-sensing indentation instruments," *Journal of Materials Research*, Vol. 1(4), pp. 601-609.
- [11] Oliver, W. C. and Pharr, G. M., 1992, "An improved technique for determining hardness and elastic modulus using load and displacement sensing indentation experiments," *Journal of Materials Research*, Vol. 7, pp. 1564-1583.
- [12] Krzesinska, M., 2004, "Influence of the raw material on the pore structure and elastic properties of compressed expanded graphite blocks," *Materials Chemistry and Physics*, Vol. 87, pp. 336-344.
- [13] Coble, R. L., and Kingery, W. D., 1956, "Effect of porosity on physical properties of alumina," *Journal of the American Ceramic Society*, Vol. 39, pp. 377-385.
- [14] ASTM D 3766-86, 2002, "Standard terminology relating to catalysts and catalysis"
- [15] ASTM D 559-90, 2005, "Standard test method for bulk density by physical measurements of manufactured carbon and graphite articles"